AMSR-E/AMSR2 Unified L3 Daily 12.5 km Brightness Temperatures, Sea Ice Concentration, Motion & Snow Depth Polar Grids, Version 1

USER GUIDE

How to Cite These Data

As a condition of using these data, you must include a citation:

Meier, W. N., T. Markus, and J. C. Comiso. 2018. *AMSR-E/AMSR2 Unified L3 Daily 12.5 km Brightness Temperatures, Sea Ice Concentration, Motion & Snow Depth Polar Grids, Version 1*. [Indicate subset used]. Boulder, Colorado USA. NASA National Snow and Ice Data Center Distributed Active Archive Center. https://doi.org/10.5067/RA1MIJOYPK3P. [Date Accessed].

FOR QUESTIONS ABOUT THESE DATA, CONTACT NSIDC@NSIDC.ORG

FOR CURRENT INFORMATION, VISIT https://nsidc.org/data/AU_SI12

National Snow and Ice Data Center

TABLE OF CONTENTS

1 DATA DESCRIPTION

1.1 Parameters

This data set consists of the following gridded parameters:

- Vertical and horizontal brightness temperatures (referred to as T_b or TB in this document) for the following channels, with separate HDF-EOS5 fields for afternoon ascending orbits, morning descending orbits, and full orbit daily averages:
  - 18.7 GHz
  - 23.8 GHz
  - 36.5 GHz
  - 89.0 GHz
- Arctic and Antarctic sea ice concentration using the NASA Team 2 (NT2) algorithm, with separate fields for ascending orbits, descending orbits, and daily averages.
- Arctic sea ice concentration differences between the AMSR Bootstrap Algorithm (ABA) and the NT2 algorithm, with separate fields for ascending orbits, descending orbits, and daily averages.
- Antarctic sea ice concentration differences between the AMSR Bootstrap Algorithm (ABA) and the NT2 algorithm, with separate fields for ascending orbits, descending orbits, and daily averages.
- Arctic and Antarctic five-day snow depth over sea ice.

1.1.1 Parameter Details

Missing or out-of-bounds T_b grid cells have a value of 0. Data have a scale factor of 0.1. Multiply data values by 0.1 to obtain T_b in Kelvin (K). The valid range of T_b is approximately 50 K to 300 K.

Sea ice concentration values:

- 0: Open Water
- 1 - 100: Percent sea ice concentration
- 110: Missing data
- 120: Land

Sea ice difference values between the ABA and NT2 Algorithms:

- 0: Bootstrap sea ice concentration is equal to the NT2 concentration
- 1 - 100: Bootstrap sea ice concentration is greater than NT2 concentration
- -1 to -100: Bootstrap sea ice concentration is less than NT2 concentration
- 110: Missing data
- 120: Land

Snow depth over sea ice values for five day running average.

- 110: Missing data
- 120: Land mask
- 130 Open water
- 140 Multiyear sea ice
- 150 Variability in snow depth
- 160 Snowmelt

1.2 File Information

1.2.1 Format

Data are in HDF-EOS5 format. For software and more information, visit the HDF-EOS website.

1.2.2 File Contents

Sample Data Images

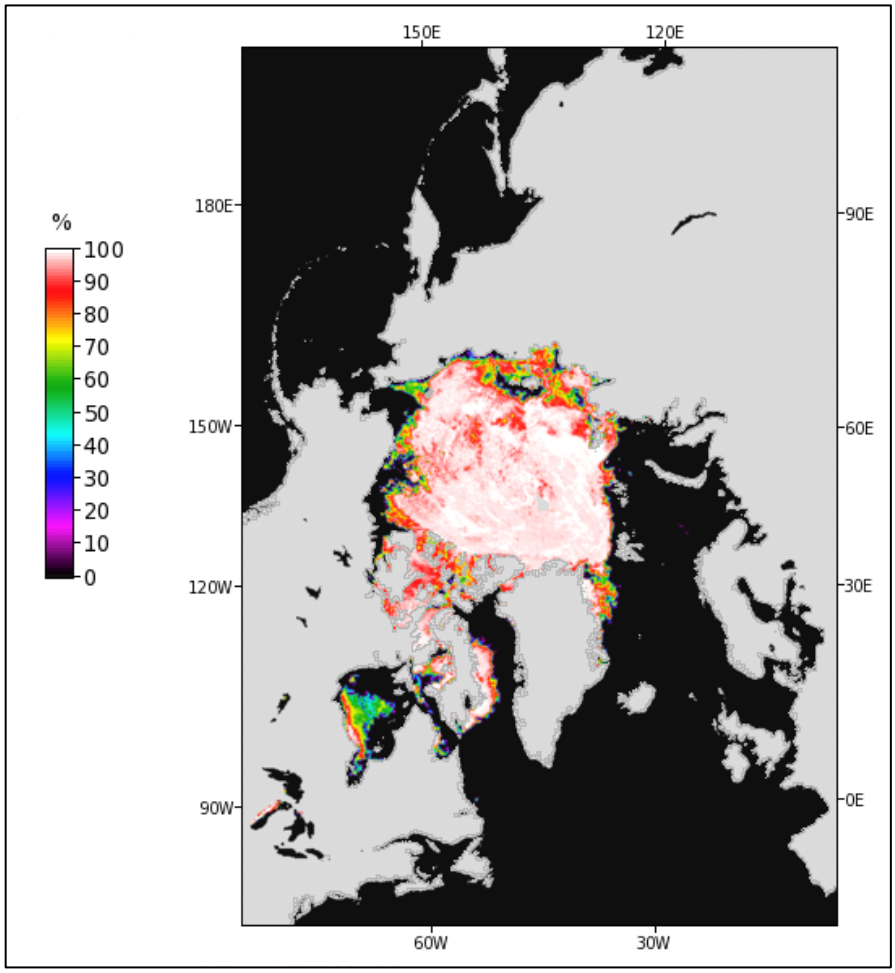

Figure 1. This Land, Atmosphere Near real-time Capability for EOS (LANCE) image shows AMSR2 Northern Hemisphere 12.5 km Sea Ice Concentration for 05 July 2016.

1.2.3 Directory Structure

Each data file includes 62 parameter fields (31 Northern Hemisphere and 31 Southern Hemisphere), and three metadata fields (CoreMetadata, StructMetadata and Processing_Facility) in 32-bit signed integer format. The figure below shows a subset of the parameter fields.

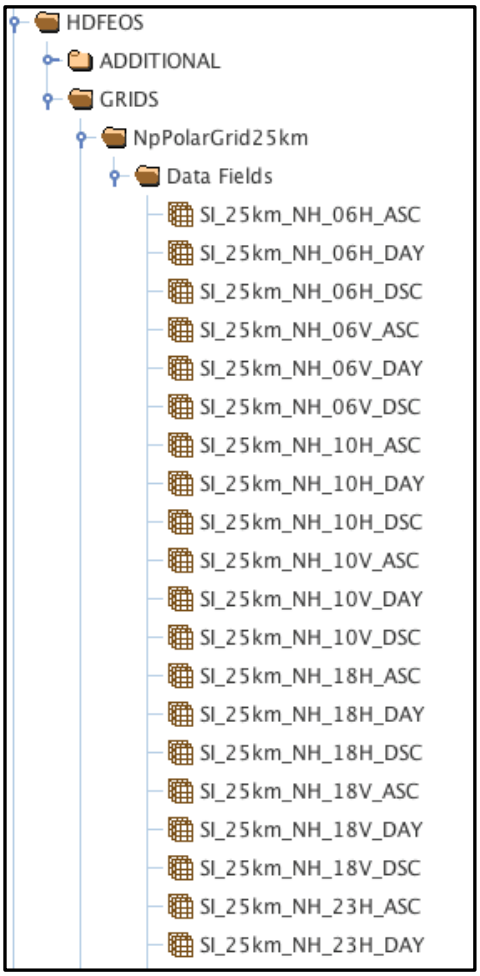

Figure 2. A subset of the Northern Hemisphere parameter fields.

1.2.4 Sea Ice Motion Data Location

Sea ice motion data in this data set are housed under the parameter “motion” in text ASCII format within the HDF file. Unlike other data in the data set, the sea ice motion data are not gridded and are therefore not plottable by standard HDF readers. The “motion” parameter contains a two-row header.

The first row indicates the two input files used for the motion correlation. Because motion is derived by cross-correlation between two gridded brightness temperature fields separated by one day, two conservative days are used.

The second row contains five values corresponding to: (1) the total motion samples in the file; (2) the number 1 as a dummy variable; (3) the number of columns in the grid (608 for the 12.5km NH polar stereographic grid); and (5) the final value which can be considered another dummy variable and irrelevant for this data.

The sea ice motion data are located beneath the two-row header. There are five columns as explained below:

Table 1. Description of Columns in the "Motion" Parameter

Column	Description
1	X-coordinate in AMSR2 polar stereographic 12.5 km grid
2	Y-coordinate in AMSR2 polar stereographic 12.5 km grid
3	U-component of motion in cm/s (in the x-direction)
4	V-component of motion in cm/s (in the y-direction)
5	Correlation value of the feature matching (values range from 0 to 1, where higher values show a stronger correlation between features and suggests more confidence in the motion estimate)

1.2.5 Naming Convention

Example 1: `AMSR_U2_L3_SeaIce12km_X##_yyyymmdd.he5`

Table 2. File Name Variables

Variable	Description
`AMSR`	Advanced Microwave Sounding Radiometer
`U`	Unified
`2`	AMSR2
`L3`	Level-3

Variable	Description
12km	Indicates each grid cell has a nominal resolution of 12.5 km x 12.5 km
X##	Product Maturity Code and Version
yyyy	Four-digit year
mm	Two-digit month
dd	Two-digit day
he5	Indicates HDF-EOS5 file format

Example 2: `AMSR_U2_L3_SeaIce25km_B01_20180509.he5`

Table 3. Product Maturity Codes

Variables	Description
B	Beta: Indicates a developing algorithm with updates anticipated.
T	Transitional: Indicates the period between Beta and Validated where the product is past the Beta stage, but not quite ready for validation. At this stage the algorithm matures and stabilizes.
V	Validated: Products are upgraded to Validated once the algorithm is verified and validated by the science team. Validated products have an associated validation stage. Refer to the Naming Conventions section of the AMSR Unified | Version History page for a description of the stages.

1.3 Spatial Information

1.3.1 Coverage

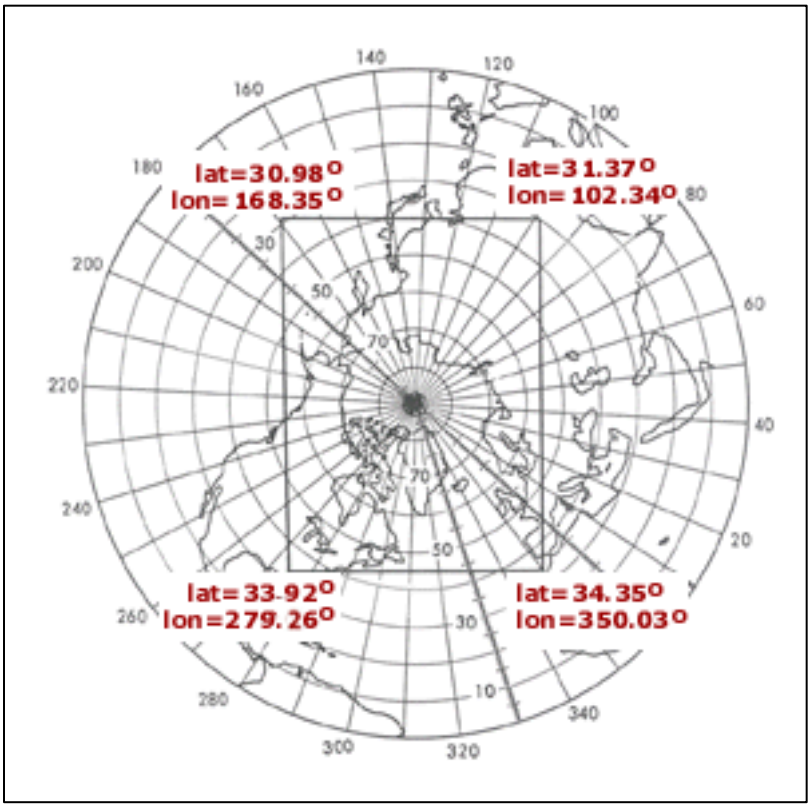

Figure 3. Northern Hemisphere Coverage Extent

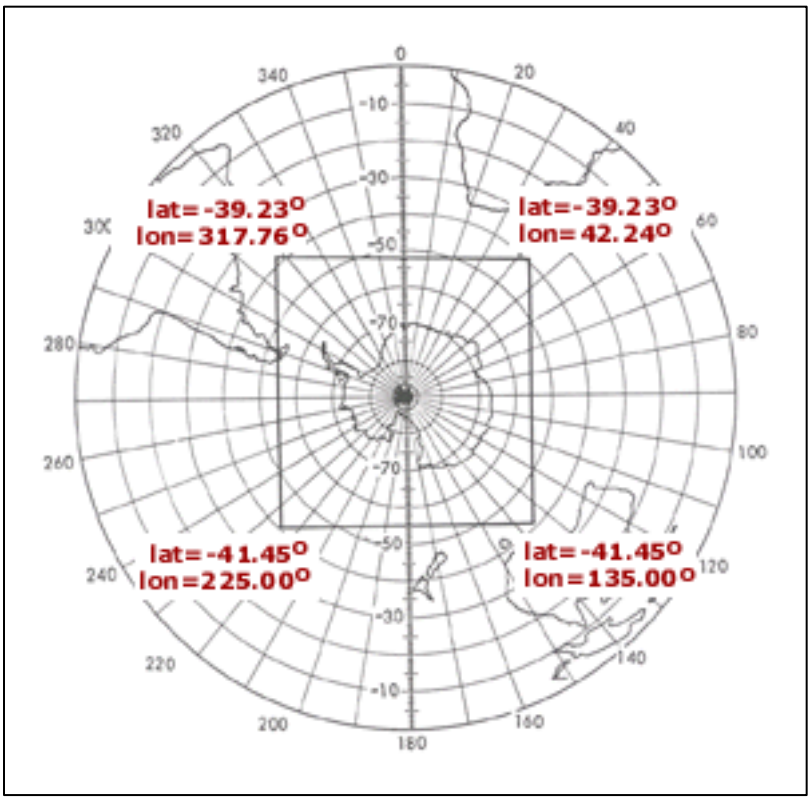

Figure 4. Southern Hemisphere Coverage Extent

A small gap in coverage exists at the poles due to the path of the ascending and descending orbits. Known as the pole hole, this gap is consistent for both AMSR2 and AMSR-E data sets. For additional information see the AMSR-E Pole Hole page.

1.3.2 Resolution

The nominal spatial resolution of the polar grids is 12.5 km. However, because the polar grids are not equal area, the actual resolution varies by latitude.

1.3.3 Geolocation

The following tables provide information for geolocating this data set:

Table 4. Projection Details

	Northern Hemisphere	Southern Hemisphere
Geographic coordinate system	Hughes 1980	Hughes 1980
Projected coordinate system	NSIDC Sea Ice Polar Stereographic North	NSIDC Sea Ice Polar Stereographic South
Longitude of true origin	0	0
Latitude of true origin	70° N	70° S
Scale factor at longitude of true origin	1	1
Datum	Hughes 1980	Hughes 1980
Ellipsoid/spheroid	Hughes 1980	Hughes 1980
Units	Meter	Meter
False easting	0	0
False northing	0	0
EPSG code	3411	3412
PROJ4 string	+proj=stere +lat_0=90 +lat_ts=70 +lon_0=-45 +k=1 +x_0=0 +y_0=0 +a=6378273 +b=6356889.449 +units=m +no_defs	+proj=stere +lat_0=-90 +lat_ts=-70 +lon_0=0 +k=1 +x_0=0 +y_0=0 +a=6378273 +b=6356889.449 +units=m +no_defs
Reference	http://epsg.io/3411	http://epsg.io/3412

Table 5. Grid Details

	Northern Hemisphere	Southern Hemisphere
Grid cell size (x, y pixel dimensions)	12.5 km	12.5 km
Number of rows	448	332
Number of columns	304	316
Geolocated lower left point in grid	-3850 E, -5350 N	-3950 E, -3950 S
Nominal gridded resolution	25 km	25 km
Grid rotation		
ulxmap – x-axis map coordinate of the center of the upper-left pixel (XLLCORNER for ASCII data)	-3850	-3950
ulymap – y-axis map coordinate of the center of the upper-left pixel (YLLCORNER for ASCII data)	5850	4350

The origin of each x, y grid is the pole. The tables below show the approximate outer boundaries for the Arctic and Antarctic grids. Corner points are listed starting from the upper left corner and progress clockwise. Interim rows define boundary midpoints.

Table 6. Arctic Grid Boundary Details

X (km)	Y (km)	Latitude (deg)	Longitude (deg)	Pixel Location
-3850	5850	30.98	168.35	corner
0	5850	39.43	135.00	midpoint
3750	5850	31.37	102.34	corner
3750	0	56.35	45.00	midpoint
3750	-5350	34.35	350.03	corner
0	-5350	43.28	315.00	midpoint
-3850	-5350	33.92	279.26	corner
-3850	0	55.50	225.00	midpoint

Table 7. Antarctic Grid Boundary Details

X (km)	Y (km)	Latitude (deg)	Longitude (deg)	Pixel Location
-3950	4350	-39.23	317.76	corner
0	4350	-51.32	0.00	midpoint
3950	4350	-39.23	42.24	corner
3950	0	-54.66	90.00	midpoint
3950	-3950	-41.45	135.00	corner
0	-3950	-54.66	180.00	midpoint
-3950	-3950	-41.45	225.00	corner
-3950	0	-54.66	270.00	midpoint

1.3.4 Geolocation Tools

NSIDC provides geolocation tools for polar stereographic data sets. NSIDC provides geolocation tools for polar stereographic data sets. See the Polar Stereo Tools page for more details.

1.3.5 Land Masks

This sea ice product utilizes a 12.5 km Northern Hemisphere land mask called amsr_gsfc_12n.hdf and a 12.5 km Southern Hemisphere land mask called amsr_nic_12s.hdf.

1.4 Temporal Information

1.4.1 Coverage

The temporal coverage of this data set extends from 02 July 2012 to the present.

1.4.2 Resolution

Brightness temperatures, sea ice concentrations and sea ice concentration difference fields are provided in three daily-averaged composites: daily averaged ascending orbits, daily averaged descending orbits, and daily average of all orbits. The snow cover fields are 5 day running averages.

2 DATA ACQUISITION AND PROCESSING

2.1 Background

Passive microwave radiation is naturally emitted by the Earth's surface and overlying atmosphere. This emitted energy is a complex function of the microwave radiative properties of the emitting body. However, for the purposes of microwave remote sensing the relationship can be described as a simple function of the physical temperature (T) of the emitting body, and the emissivity (ε) of the body.

$Tb = \varepsilon * T$ (Equation 1)

Brightness temperature (T_b in Kelvin) is the parameter retrieved by satellite sensors (after calibrations), and is the input parameter to passive microwave sea ice concentration algorithms.

Passive microwave data are particularly useful for sea ice studies because of the high contrast in emissivity between open water and sea ice. This contrast is dependent on the frequency and polarization of the microwaves; the contrast between water and ice is generally higher at lower microwave frequencies and at horizontal polarizations.

Due to sea ice surface complexities, atmospheric emission, and scattering; direct physical relationships between the microwave emission and the physical sea ice concentration are complex and not easily connected. Thus, the standard approach is to estimate concentration through empirical relationships; i.e., concentration is derived from examining the characteristics of the data themselves.

These empirically-derived algorithms take advantage of the fact that T_b in microwave frequencies tend to cluster around consistent values for pure surface types (100% water or 100% sea ice). Concentration can then be derived using a simple linear mixing equation (Zwally et al., 1983) for any T_b that falls between the two pure surface values:

$Tb = TICI + TO(1-CI)$ (Equation 2)

Where T_b is the observed brightness temperature, T_i is the brightness temperature for 100% sea ice, T_O is the brightness temperature for open water, and C_I is the sea ice concentration.

In reality, such an approach is limited by surface ambiguities and atmospheric emission. Using combinations of more than one frequency and polarization limits these effects, resulting in better discrimination between water, and different ice types, as well as a more accurate concentration estimate

2.2 Acquisition

This product is derived using Japan Aerospace Exploration Agency (JAXA) AMSR2 Level-1R input T_b observations from T_b channels; 6.9, 10.7, 18.7, 23.8, 36.5 and 89 GHz. For the sea ice parameters, The JAXA AMSR2 T_b observations are adjusted (intercalibrated) to match the JAXA AMSR-E T_b observations, thus enabling consistent geophysical parameters to be obtained across the JAXA AMSR2 and AMSR-E products.

Note that the AMSR-E products at the National Snow and Ice Data Center (NSIDC) currently only use the Level-2A T_b observations provided by Remote Sensing Systems. In the future AMSR-E T_b observations may be reprocessed with the unified JAXA Level-1R T_b observations and archived at NSIDC.

The Level-1R input data are resampled T_bs. The T_b sensor footprints (instantaneous field of view) vary with frequency. The resampling remaps the T_bs to sets of consistent footprint sizes using the Backus-Gilbert method (Backus et al. 1967). Each resampled set corresponds to the footprint of one frequency and contains that frequency plus all higher-resolution frequencies. Therefore, the number of channels in each resampled set of T_bs varies. See JAXA Level 1R documentation or Maeda et al. 2016 for more information.

Observations for the 6.9, 10.7, 18.7, 23.8, 36.5, and 89 GHz channels, at resampled resolutions, from the JAXA L1R data are gridded into 12.5 km grid cells using a drop-in-the-bucket method where the grid cell that contains the center of the observation footprint is given the whole weight of the observation. With this procedure, the number of observations is always in whole numbers. All valid T_b observations within the extent of the polar grids are binned into grid cells, including land observations. Note that the NASA Team 2 sea ice concentration algorithm is run on the L1R swath data and then gridded into ascending, descending, and daily average grids using the same procedure as the gridded T_b and other parameters.

2.3 Processing

2.3.1 Intercalibration

The sea ice algorithms for AMSR2 are the same as those used for AMSR-E. The only substantial difference is that AMSR2 T_bs are adjusted (intercalibrated) to match AMSR-E T_bs, so that the algorithm coefficients can remain the same and obtain consistent geophysical estimates across both AMSR-E and AMSR2.

An intercalibration was performed across common points of AMSR2 and slow rotation AMSR-E T_bs. Regressions were performed for these common points over a full year and averaged to

develop regression equations to adjust AMSR2 T_bs into T_bs consistent with the AMSR-E algorithms.

Overall, the regressions showed very good consistency between AMSR2 and the slow-rotation AMSR-E. The most notable difference is found in the 18 GHz V polarization channel, which has slopes slightly off from 1 and higher intercept values. The 89 GHz channels also show less agreement than the other channels, likely due to the greater atmospheric emission at 89 GHz. The average regression and correlation coefficients used in the AMSR2 processing are provided in Table 1 of the AMSR2 Sea Ice Algorithm Theoretical Basis Document (ATBD), Meier et al. 2017. These regression equations are applied to the AMSR2 T_bs before they are fed into the subsequent geophysical algorithms.

2.3.1.1 Algorithm

The 12.5 km sea ice concentration product is generated using the Enhanced NASA Team (NT2) algorithm described by Markus et al. 2000 and Markus et al. 2009 for both the Arctic and the Antarctic. The NT2 algorithm uses two ratios of brightness temperatures: polarization ratio (PR) and spectral gradient ratio (GR). These ratios are calculated using the following two equations:

$$PR(v) = [TB(vV) - TB(vH)] / [TB(vV) + TB(vH)]$$ (Equation 3. Polarization Ratio)

$$GR(v1pv2p) = TB(v1p) - TB(v2p)] / [TB(v1p) + TB(v2p)$$ (Equation 4. Spectral Gradient Ratio)

where TB is the brightness temperature at frequency v for the polarized component p (vertical V or horizontal H).

The NT2 Algorithm uses these ratios to identify two ice types for the Arctic and Antarctic. In the Arctic, the two ice types correspond to first year ice and multiyear ice. Multiyear ice represents sea ice with a heavy snow cover resulting in increased scattering. In the Antarctic, there is little multiyear ice and the two ice types represent regimes of snow-covered sea ice. The distribution of these ice types is shown in Figure 1 (top section) of the ATBD.

The primary source of error in the original NASA team algorithm was attributed to conditions in the surface layer such as surface glaze and layering (Comiso et al. 1997), which can significantly affect the horizontally polarized 19 GHz T_b (Matzler et al. 1984) leading to increased PR(19) values and thus an underestimate of ice concentration. The use of horizontally polarized channels makes it imperative to resolve a third ice type to overcome the difficulty of these surface effects on the emissivity of the horizontally polarized component of the T_b.

GR(89V19V) and GR(89H19H) are gradient ratios used to resolve the ambiguity between pixels with low ice concentration and pixels with significant surface effects. The difference between these two GRs (ΔGR) is used as a measure of the magnitude of surface effects. Based on this analysis a new ice type is introduced (Type C) which represents ice having significant surface effects; see Figure 1 (bottom section) in the ATBD.

The NT2 algorithm includes an atmospheric correction scheme as an inherent part of the algorithm. The response of the T_bs. to different weather conditions is calculated using an atmospheric radiative transfer model, (Kummerow et al. 1993). Input data for the model are the emissivities of first-year sea ice under winter conditions taken from Eppler et al. 1992, with modifications to achieve agreement between modeled and observed ratios.

Atmospheric profiles are used as another independent variable in the algorithm. There are twelve profiles that include different cloud properties such as cloud base, cloud top, cloud liquid water (Fraser et al. 1975), and average atmospheric temperatures and humidity profiles for summer and winter. The profiles are combined with the radiative transfer model to develop a look-up table of T_b values corresponding to all concentrations (0-100% in 1% intervals) of the two ice types for each of the twelve atmospheric profiles. This results in a model solution space of 101x101x12, or 122,412 possible solutions.

2.3.1.2 Weather Filters

Two additional weather filters are applied to correct for severe weather effects over open ocean. These filters are based on spectral gradient ratios, and implemented using threshold values similar to those used by the NT algorithm (Gloersen et al. 1986) and (Cavalieri et al. 1995). Figure 5 of the ATBD shows sea ice concentration maps with and without atmospheric correction.

A final weather filter is applied to correct for residual weather contamination particularly at low latitudes. This filter is based on monthly climatological sea surface temperatures (SSTs) from the National Oceanic and Atmospheric Administration (NOAA) ocean atlas. In the Northern Hemisphere, any pixel where the monthly SST is greater than 278 K is set to zero; whereas in the Southern Hemisphere, any pixel where the monthly SST is greater than 275 K is set to zero.

2.3.1.3 Land Spillover Correction

The spillover of land classified pixels and water classified pixels leads to erroneous ice concentrations along the coast lines adjacent to open water. This makes operational usage of these maps cumbersome. To overcome this difficulty a five-step pixel classification scheme is applied to delineate land pixels from water pixels. See section 3.2.1.2 and Figure 4 of the ATBD for a detailed description of the classification process, and to view ice concentration maps; with and without land spillover correction.

2.3.1.4 Processing Steps

1. Calculate sea ice concentration: Brightness temperature values are calculated for each ice concentration and weather combination, and for each of those solutions the ratios PRR (19), PRR (89), and ΔGR are calculated. The three observed ratios are then compared with the three modeled ratios. The indices where the differences are smallest will determine the final ice concentration combination.
2. Distinguish new ice from existing ice with surface effects: Gradient ratio (37V19V) with a threshold of –0.02 is used to resolve type C ice for pixels where GR(37V19V) is below this threshold, or thin ice for pixels where GR(37V19V) is above this threshold.
3. Apply weather filters: To eliminate severe weather effects over open ocean, weather filters based on the spectral gradient ratio are applied. The threshold for the GR(37V19V) NT weather filter (Gloersen and Cavalieri 1986) is 0.05, where the threshold for the GR(22V19V) NT weather filter (Cavalieri et al. 1995) is 0.045. If the GR values exceed these thresholds, the sea ice concentrations are set to zero.
4. Map sea ice concentration values into daily gridded fields: After the algorithm is run on JAXA L1R T_bs, swath concentrations are mapped on to a polar stereographic grid, and three daily fields for ascending passes, descending passes, and daily averages are created. The gridding of the concentration fields is done using the same drop-in-the-bucket process as the other gridded products.
5. Apply sea surface temperature (SST) filters: To eliminate low-latitude spurious ice concentrations, Sea Surface Temperatures (SST) filters based on the National Oceanic and Atmospheric Administration (NOAA) monthly ocean atlas are applied. In the Northern Hemisphere, ice concentration is set to zero, where SST is greater than 278 K. In the Southern Hemisphere, ice concentration is set to zero, where SST is greater than 275 K.
6. Apply land spillover mask: A land spillover correction scheme is applied to correct for erroneous ice concentrations along coast lines. This scheme utilizes a five-step pixel classification method to distinguish coastline from sea ice.

For a detailed description of the Algorithm processing for this dataset refer to the ATBD document.

2.3.2 Derivation Techniques for Sea Ice Concentration Difference

The AMSR Bootstrap Algorithm (ABA; Comiso, Cavalieri and, Markus 2003) is used in the calculation of sea ice concentration differences between the ABA and the NT2 (ABA-NT2) for both hemispheres. The ABA uses 6.9 GHz data to reduce temperature effects on 18.7 GHz and 36.5 GHz T_bs., which provides similar results to those of the Bootstrap Basic Algorithm (BBA) used in the 12.5 km sea ice product.

2.3.3 Derivation Techniques for Snow Depth on Sea Ice

The AMSR-E snow-depth-on-sea-ice algorithm was developed using DMSP SSMI data (Markus and Cavalieri 1998) to estimate snow depth on sea ice from space. The snow depth on sea ice is calculated using the spectral gradient ratio of the 18.7 GHz and 37 GHz vertical polarization channels,

```
hs = a1 + a2 GRV(ice)
```

where hs is the snow depth in meters, and a1 = 2.9 and a2 = -782 are coefficients derived from the linear regression of in situ snow depth measurements on microwave data. GRV(ice) is the spectral gradient ratio corrected for the sea ice concentration, C, as follows

```
GRV(ice) = [TB(37V)-TB(19V)-k1(1-C)] / [TB(37V)+TB(19V)-k2(1-C)]
```

with `k1=TBO(37V)-TBO(19V)` and `k2=TBO(37V)+TBO(19V).` The open water brightness temperatures, TBO, are average values from open ocean areas and are used as constants. The principal idea of the algorithm (Kelly et al. 2003) is based on the assumptions that scattering increases with increasing snow depth and that the scattering efficiency is greater at 37 GHz than at 19 GHz. For snow-free sea ice, the gradient ratio is close to zero and it becomes more and more negative as the snow depth (and grain size) increases. The correlation of regional in situ snow depth distributions and satellite-derived snow depth distributions is 0.81. The upper limit for snow depth retrievals is 50 cm, which is a result of the limited penetration depth at 18.7 and 36.5 GHz.

The algorithm is applicable to dry snow conditions only. At the onset of melt, the emissivity of both the 18.7 GHz and the 36.5 GHz channels approach unity (that of a blackbody) and the gradient ratio approaches zero initially before becoming positive. Thus, snow depth is indeterminate under wet snow conditions. Snow, which is wet during the day, frequently refreezes during the night. This refreezing results in very large grain sizes (Colbeck 1982), which leads to a reduced emissivity at 36.5 GHz relative to 18.7 GHz, thereby decreasing GRV(ice) and thus leads to an overestimate of snow depth. These thaw-freeze events cause large temporal variations in the snow depth retrievals. This temporal information is used in the algorithm to flag the snow depths as unretrievable from those periods with large fluctuations.

As in situ grain size measurements are even less frequently collected than snow depth measurements, the influence of grain size variations could not be incorporated into the algorithm. Because of the uncertainties in grain size and density variations as well as sporadic weather effects, AMSR2 daily snow depth products are five-day running averages similar to the AMSR-E snow depth on land product.

Snow depths are retrieved for the entire Southern Ocean, but only for the seasonal sea ice zones in the Arctic. This is due to the fact that Arctic snow depth is complicated by the presence of multiyear ice, which has a signature similar to snow cover on first-year ice. Both multiyear ice and deep snow on top of first-year ice results in increasingly negative values for the spectral GR; therefore, the algorithm only retrieves snow depth in the seasonal sea ice zones and in regions where the value of GR(37V19V) is greater than -0.02. This threshold corresponds to multiyear ice concentration of less than 20 percent. Where GR(37V19V) is less than -0.02 threshold used by the

algorithm to flags pixels as multiyear ice. Because of the higher sensitivity of snow depth retrievals to ice concentration less than 20 percent, the algorithm limits snow depth retrievals to ice concentration between 20 -100 percent. Ice concentrations less than 20 percent appear almost exclusively near the ice edge. The following image summarizes the processing sequence for the snow depth algorithm.

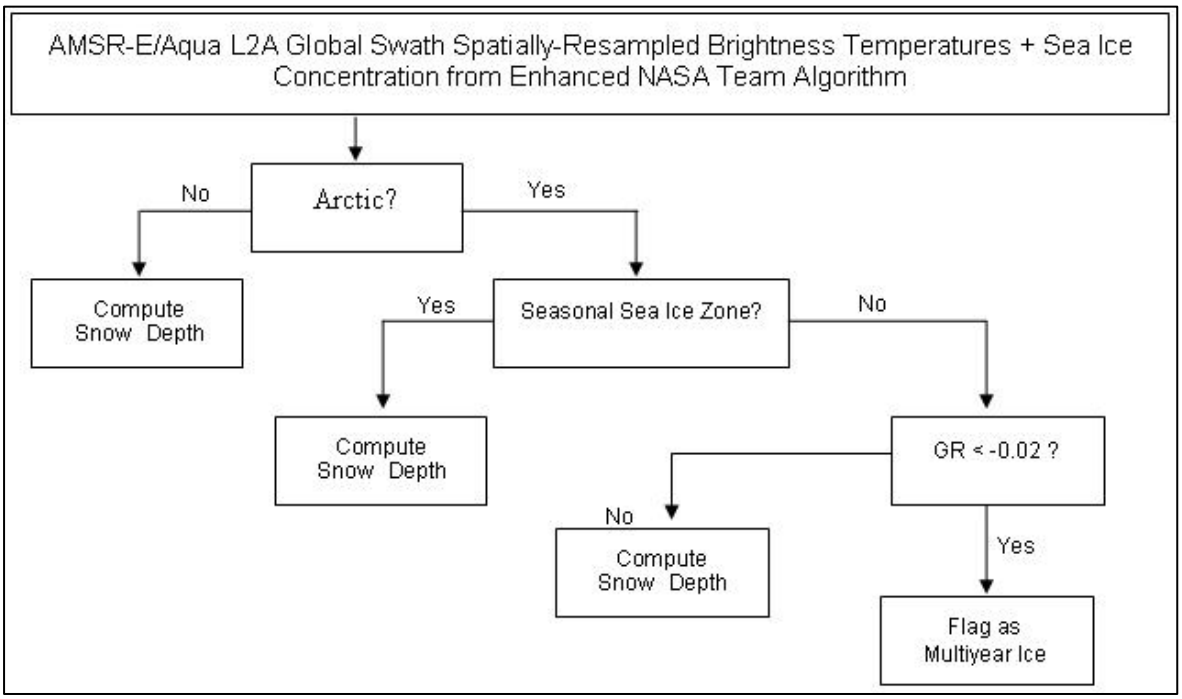

Figure 5. Snow depth processing sequence from the NASA Team Algorithm.

2.3.4 Derivation Techniques for Sea Ice Drift

The method to estimate sea ice drift is the Maximum Cross-Correlation feature-tracking algorithm developed at the University of Colorado (CU) (Emery et al., 1995). The basic methodology of the algorithm is fairly simple. Two spatially coincident images are obtained, separated by some period of time. A target area, which may be defined by a pixel or a group of pixels, is chosen in the first (older) image. Then, a search area surrounding the target area is chosen in the second (newer) image. Correlations with the target area in the first image are compared with all regions (of the target area's size) in the search area of the second image. The region with the highest correlation is determined to be the location where the target moved. A filtering algorithm is then employed to remove at least some of the questionable matches.

Gridded Level 3 daily composite T_bs at 12.5 km on the polar stereographic grid are used as input for the motion algorithm. Ice motions are calculated from two composite images using the sliding window to find the correlation peak, which determines the distance a feature has moved. The drift is then computed by dividing the distance by the time separation (24 hours). A sea ice mask is

applied to only retrieve ice motion where concentration is above the standard sea ice extent threshold of 15% concentration. False correlations can occur due to clouds or variability of ice surface features. To eliminate this, first a minimum correlation threshold of 0.7 is applied to eliminate weak matches. Next a post-processing filter program is run to remove at least some questionable and erroneous motions. This uses the fact that motion is highly spatially correlated and requires that each vector be reasonably consistent in speed and direction with at least two neighboring motion estimates.

2.3.5 Processing Summary

The figure below summarizes the input sources and algorithms used to create the gridded AMSR2 12.5 km sea ice concentration, sea ice difference and snow depth on sea ice products.

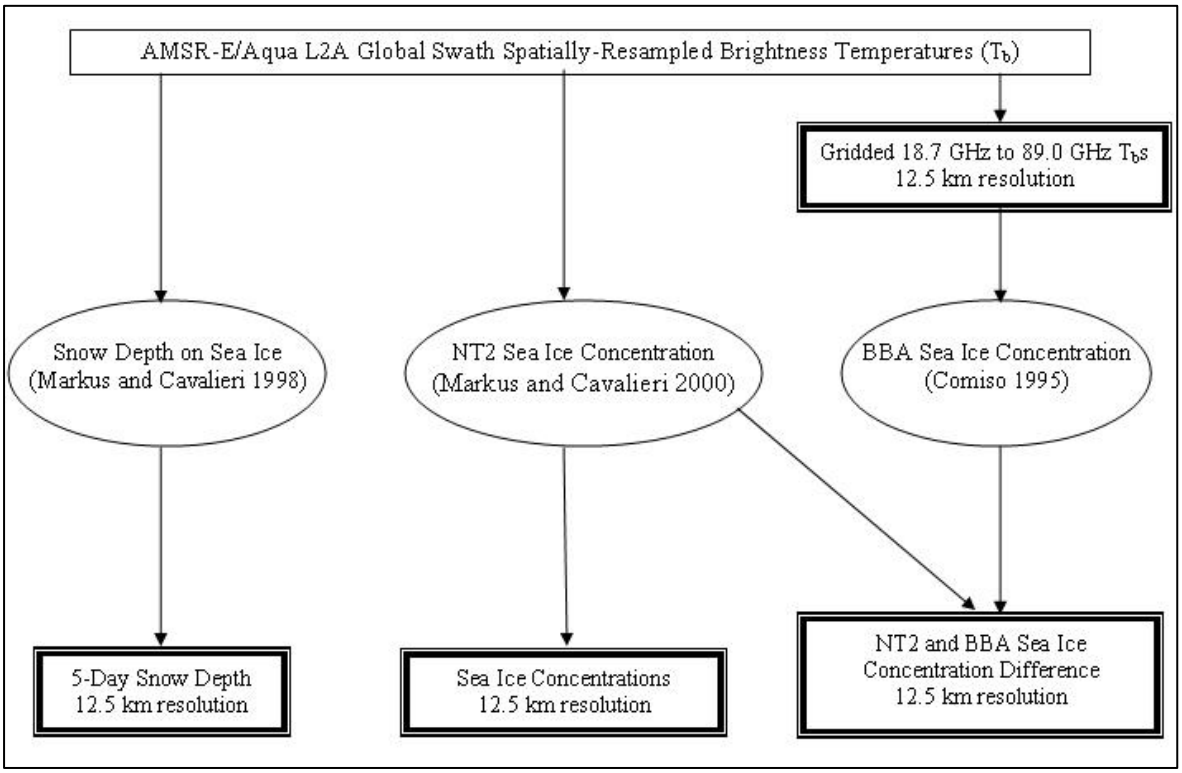

Figure 6. Processing sequence for creating AMSR-E and AMSR2 12.5 km sea ice products.

3 DOCUMENT INFORMATION

3.1 Publication Date

09 July 2018

3.2 Date Last Updated

March 2022